

# A Tiltable Airframe Multirotor UAV Designed for Omnidirectional Aerial Manipulation

Hannibal Paul, Ricardo Rosales Martinez, Borwonpob Sumetheeprasit and Kazuhiro Shimonomura

**Abstract**—Aerial manipulators coupled to UAVs can be beneficial for doing tasks in difficult-to-reach areas. Inspection is one of such most commonly required tasks conducted on aging infrastructure including bridges and tunnels. However, while employing an inspection UAV, the manipulator tip's angle of reach is often mechanically limited to only about the location of its attachment on the aircraft. In the proposed system, a design that allows a manipulator tip to reach all directions surrounding the UAV is developed. As the manipulator body, we propose a basic tiltable airframe design and employ auxiliary actuators to maintain the rotors' axis. The thrust direction of the rotors remains upright in the proposed design, which allows the rotor thrust to hold the maximum payload of the UAV even while tilted. We examine its efficiency and usefulness through experimental demonstration.

## I. INTRODUCTION

Unmanned aerial vehicles (UAV), specifically multirotors, are evidently a useful platform for aerial manipulation due to its mobility and hovering capability [1]. One of the main advantage of UAV is reaching places that are normally hard for a person to reach. Using such a robotic system allows us to reach places that are highly elevated and difficult to access. Construction [2], inspection and maintenance by reaching the underside of bridges [3], high voltage power-lines [4], large chemical tanks, facade inspection of buildings [5], and other locations are among the tasks. In such cases, adding a manipulator system to a UAV to perform aerial manipulation or inspection tasks is more time and cost efficient compared to construction of the scaffolding. Furthermore, the necessity and risk to human workers to work in such dangerous place is reduced.

The subject of aerial manipulation has lately been expanding, with many types of manipulator systems being designed to fit on a UAV [6]. The type of task that can be accomplished in various locations by physical interaction, is determined by the type and number of manipulators [7], and its location on-board the UAV [8]. Due to the mechanical limitations, the aerial manipulators can only interact with the surrounding surface from the position of their attachment on the UAV. This makes it difficult to employ in applications such as examining tunnel walls and ceilings or complex structures using single system. Attaching multiple manipulators around UAV is an option [9], however deploying them for a particularly specialized purpose like inspection, may make the system bulky. In such instances, it would be advantageous if

the same manipulator's tip could reach numerous locations around the UAV's frame [10]. Frames with tiltable rotor designs, on the other hand, allow the UAV to hover in place even when the airframe is tilted, which is an intriguing recent development in aerial manipulation [11]. However, using such a design complicates the system's structure, and the thrust required to maintain the UAV's maximum payload must be increased if the rotor itself is tilted.

In our proposed design, we use a tilting airframe structure similar to the tiltable rotor concept, but the rotors' axis remain upright. The benefit of such design is that the control of the UAV will remain the same even after tilting. The only difference is a minor offset between the rotors and their heights when the airframe is controlled to tilt. By extending attachments on both ends of the tilting airframe, it may be utilized as the body of a manipulator, allowing it to reach multiple angles during flight as shown in Fig. 1. The system may be used to inspect high walls, ceilings, slanted surfaces and curved structures with suitable additional attachments.

## II. TILTABLE AIRFRAME MANIPULATOR

A UAV-based inspection may collect data faster than a human and eliminates the need for scaffolding, which may be costly and time-consuming to construct and dismantle, increasing costs through longer downtimes. When executing this sort of operation, using a UAV to collect inspection data reduces personal injuries. Thickness measurement is one of the most important inspection tasks in the industrial and

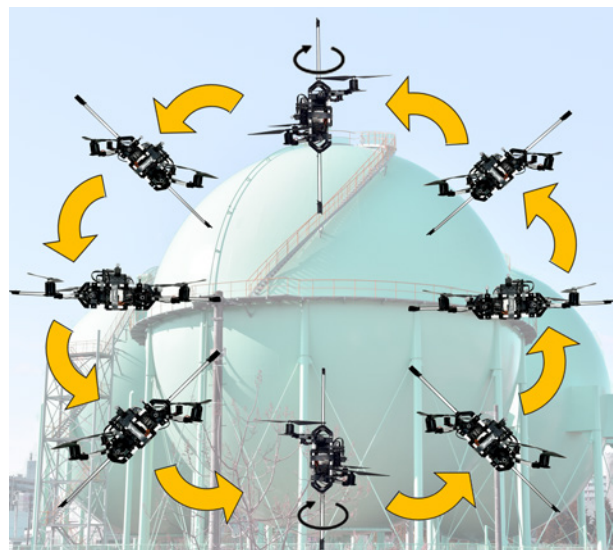


Fig. 1: Concept of omnidirectional aerial physical contact on a spherical gas tank, using tiltable airframe UAV.

Department of Robotics, Graduate School of Science and Engineering, Ritsumeikan University, Kusatsu 525-8577, Japan  
hpaul@fc.ritsumei.ac.jp, skazu@fc.ritsumei.ac.jp

transportation industries for keeping track of corrosion [12]. In such cases, a UAV must maintain a certain amount of force on the surface being tested and stay in contact for the duration of the sampling [13].

Moreover, in most of the manipulation or inspection cases, a robot needs to exert or maintain certain amount of force on the target [14]. In case of conventional multirotor UAVs, the rotors and their propellers are mounted horizontal to the airframe, and the thrust forces generated are parallel to each other. The thrust force of each rotor and their reaction torque due to rotor drag are given by

$$\begin{aligned} f_i &= \mu\omega_i^2 \\ \tau_{zi} &= f_i k_i \end{aligned} \quad (1)$$

Where  $\mu$  and  $k$  refer to the lift force and aerodynamic drag coefficient respectively, and  $\omega$  to the angular velocity of the motors. In order to move side-wards, the speed of appropriate motors are controlled to orientate the frame and move in the tilted direction. During tilt, the rotors need to spin faster to also maintain the current altitude, compared to simply hovering horizontally. The magnitude of the forces that act on the center of mass (CoM) and the moments generated by this forces, control the orientation and motion of system. Considering a planar rotor configuration of Fig 2, where the rotors named  $M1, M2$  spin in the counter clockwise direction and  $M3, M4$  in the clockwise, the forces and moments can be expressed as,

$$\begin{bmatrix} f_x \\ \tau_x \\ \tau_y \\ \tau_z \end{bmatrix} = \begin{bmatrix} 1 & 1 & 1 & 1 \\ y_1 & -y_2 & y_3 & -y_4 \\ -x_1 & x_2 & x_3 & -x_4 \\ k & k & -k & -k \end{bmatrix} \cdot \begin{bmatrix} f_1 \\ f_2 \\ f_3 \\ f_4 \end{bmatrix} \quad (2)$$

where,  $f_1, f_2, f_3$  and  $f_4$  correspond to the forces generated by rotors  $M1, M2, M3$  and  $M4$  respectively. The values of  $x_1, x_2, x_3$  and  $x_4$  refer to the distance in the x axis from the CoM to the corresponding rotor. Whereas  $y_1, y_2, y_3$  and  $y_4$  correspond to that distance in the y axis. Applying force in a side-ward direction during aerial manipulation might reduce system efficiency and make the aircraft unstable. As a result, several studies concentrated on creating thrust-vectoring systems to apply additional force on the target [15]. Attaching additional ducted fans to apply force in the required direction, in addition to the rotors, can provide a

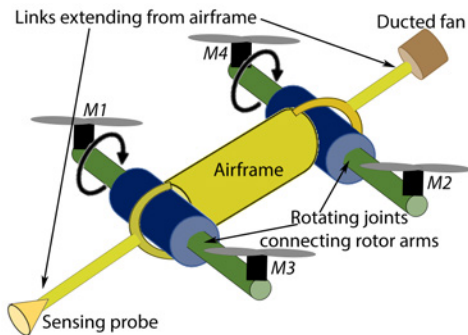


Fig. 2: A tiltable UAV based manipulator design for inspection or force application.

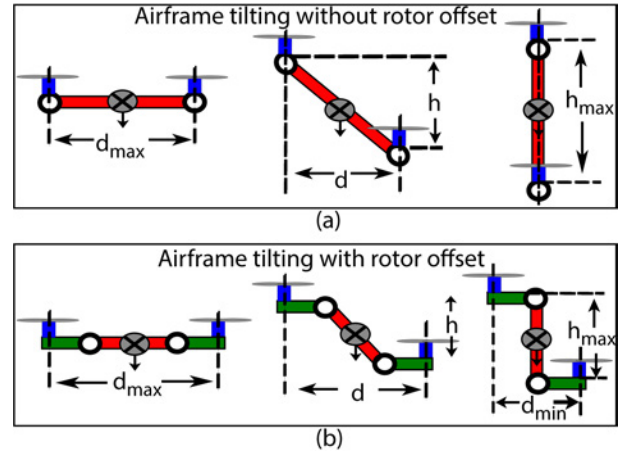


Fig. 3: Side-view of the tilting airframe UAV (a) without rotor attachment offset and (b) with rotor attachment offset.

faster response. We previously developed a high-pressure water jetting UAV for high-rise structures [16]. Additional ducted fans pointing sideways were mounted to maintain aircraft position against water jet response forces. However, the thrust generated by these fans is confined to the horizontal direction.

The purpose of this research is to develop a manipulator system for a UAV with a tilting frame, possibly for inspection. The system is primarily comprised of a manipulator body, as illustrated in Fig. 2, which is constructed of a long pipe that may be coupled with a sensor probe at one end and a ducted fan at the other end if necessary. When using the sensor probe to measure data from a surface, the ducted fan allows for the application and maintenance of constant force. For such an application, a long manipulator structure with a center tilting mechanism may be beneficial.

The current design relies on the in tandem tilting of the rotor mounted links as pairs, where the front set of rotors  $M1, M3$  and the back  $M2, M4$  follow the same angle setpoint. This type of tilting maintains the propeller's thrust force vectors parallel to each other, and constrains the CoM to be in between the actuators. The effects of the transition are of a lesser effect in respect to the trust force generated and the reaction torque of each motor, which follow (1). Due to the nature of the transition, the distance in  $y$  between the motors remain constant. As such the the moment  $\tau_x$  still follows the expression defined in (2). This is also the case for  $\tau_z$ , since the motors force vectors always remained parallel, and total force magnitude collinear to the  $z$  axis. The more significant changes occurs in regard to  $\tau_y$ , since the tilt controlled by the servo motors translates the position of the motors along the  $x$  axis, given by,

$$\tau_y = \sum_{n=1}^4 f_i x(\alpha) \quad (3)$$

Where  $x(\alpha)$  refers to the distance from the CoM to the motors thrust vectors. This distance changes based on the tilt angle  $\alpha$  of the servo motors. Fig.3 shows two possible approaches for this type of tilting with minimum thrust loss.

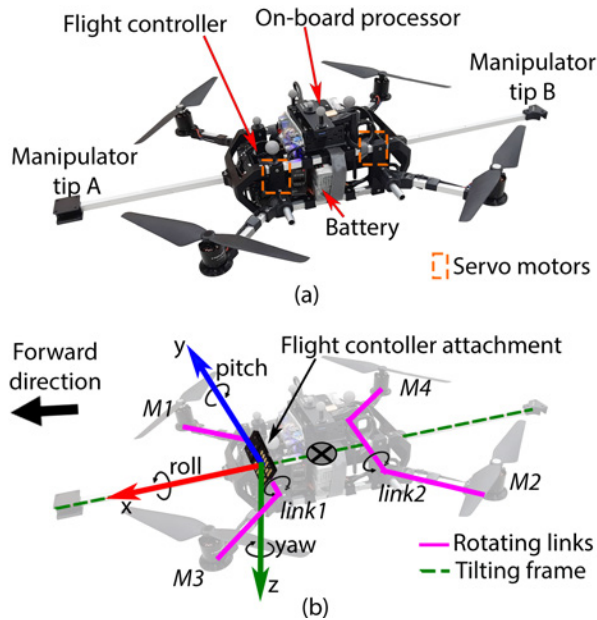


Fig. 4: Developed prototype of tiltable airframe UAV.

The first design described in Fig.3(a) shows a system that although capable of tilting, has a smaller range of stable motion when compared to Fig.3(b). Recent works of tilting frame UAV design in [17] and [18] are similar to Fig.3(a), they have no or small rotor offset, so it's difficult to make the posture of the airframe vertical. Also, [19] has a 3-axis deformable frame, but we adopted dual-axis tilting frame in order to attach the manipulator. For our design the distance  $x(\alpha)$  is defined as,

$$x = r_x \cos \alpha \quad (4)$$

Where  $r_x$  refers to the distance from the CoM to the servo motors. This is emphasized when the system is tilted to  $90^\circ$ , as shown in (c), where the severe overlapping of the propellers has undesired effects in the flight stability. Solving for (3) and (4) further expose the limitations of this design. At this configuration the position of the CoM with respect to the motors removes a degree of control, since  $\tau_y$  becomes 0. The addition of an offset between the servo motors and the propellers, removes this limitation. In this case the total distance  $x(\alpha)$  is now given by,

$$x = r_x \cos \alpha + d_{offset} \quad (5)$$

Even when the tilt angle approaches  $90^\circ$ , the offset allows the system to maintain control of its pitch angle. Moreover, the overlapping of the propellers is also reduced.

### III. DESIGN AND CONTROL

The structure the UAV consists of a tilting airframe, which is also considered as body of the manipulator. The rotors are attached on rotating links as shown in Fig. 4. Each rotating link has two rotors attached on its ends forming a quadrotor UAV when combined. The prototype is assembled using aluminium pipes and 3D printed parts. The rotating link lengths are appropriately chosen so that propellers don't hit the airframe during tilting. Two aluminium pipes are

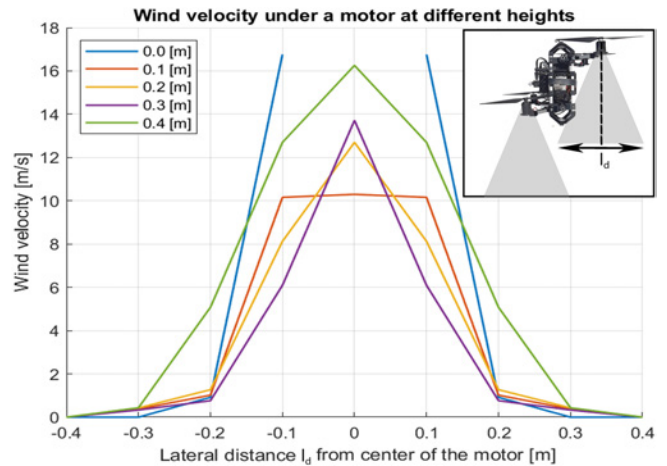


Fig. 5: Downwash profile generated by a rotor.

attached along the length of the airframe forming a long two-ended manipulator. The length of this attachment can be extended based on the requirement, but however must be at least longer than the propellers spinning range to avoid propeller crashing into an inspecting surface. In addition, sensor probes and ducted fan can be attached on the two open ends of the manipulator attachment.

The rotors are securely fastened to the rotating links. The frame can be tilted in relation to the two rotating links by utilizing a servo motor on either side. The angle of rotors  $M1$  and  $M3$  is controlled by one rotating link, while the angle of rotors  $M2$  and  $M4$  is controlled by the second link. The angle of the rotor axes can be kept parallel by adjusting the servo angles with the same magnitude and direction. During flight, the UAV attempts to maintain each rotors in upright direction. As a result, when the rotating links are activated during flight, their angle simply tilts the UAV's airframe. The tilting also causes the rotors of the associated rotational linkages to alter height.

When the aircraft is tilted, the downwash from the top propellers may alter the airflow to create thrust in the bottom propellers, and vice versa. When the frame tilt angle is  $90^\circ$ , the maximum possible propeller area overlap occurs. To analyse this, the downwash profile measurements were taken beforehand and plotted, as shown in Fig. 5. Based on the graph, we validated that the downwash from one propeller will not impact the others if the rotor spacing is large enough during tilted configuration. When the airframe is tilted to  $90^\circ$  and  $0^\circ$ , the minimum and maximum separation between rotors occur, which are utilized to estimate the link lengths.

A Pixhawk 6C flight controller is attached on front rotating link (*link1*) as shown in Fig. 4)(b). The flight controller positioning with respect to UAV's CoM is accounted for in the flight controller settings. The flight controller is attached in such a configuration, to keep the flight controller orientation in conjunction with the rotors angle. In addition, such configuration allows it to be easily fitted and rotated in a compact space inside the UAV. The developed prototype's airframe can be tilted from  $-90^\circ$  to  $90^\circ$ . Beyond this, the tip position angles can be controlled by twisting the UAV in

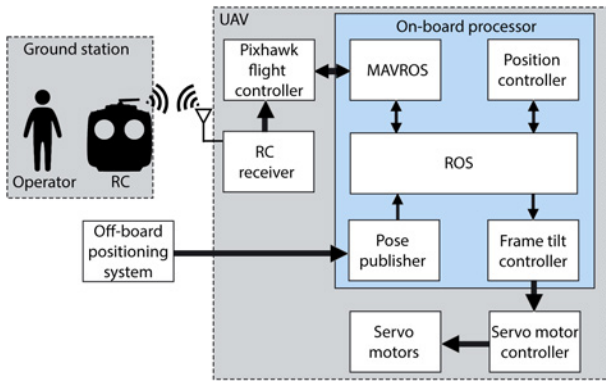


Fig. 6: Block diagram of the control system.

its yaw axis. The attitude of the UAV is always measured with respect to the flight controller’s orientation. Even when the airframe is controlled to tilt, the rotating links maintain horizontal posture, thereby keeping the flight controller’s roll and pitch angles at 0. Therefore, during flight, the rotors are being controlled to keep the angle of flight controller attached link (*link1*) horizontal. TABLE I contains the specifications of the developed prototype. Rotors with ratings of 920 Kv and a thrust of 814 g at 70% of their speed are chosen based on the UAV’s payload estimation.

An Intel UP board is used for on-board processing and control. Fig. 6 depicts the system’s communication connection and data transfer. Using a serial connection, the flight controller communicates with the on-board PC through the Mavlink protocol. Mavros, a ROS implementation of Mavlink, relays data from the flight controller to the ROS protocol. The current position estimate of the flight controller is obtained from Mavros and utilized as feedback in the position controller node. Furthermore, Mavros delivers raw RC inputs as operator commands for tilting the aircraft. The tilt controller node receives the RC inputs and processes them before communicating the command to the servo motor controller, which controls the movement of the servo motors. Two Dynamixel MX-106 servo motors, each with stall torque of 8.4 N.m at 12 V are used. The UAV’s location and orientation are provided via an off-board positioning system, which is utilized for position holding and check point following. Because of its precision and reliability, a motion capture system is utilized for position feedback in the experiments. Alternatives to motion capture, such as a tracking camera or visual odometry, can be employed in various applications. The position data is transmitted to

TABLE I: Specifications of the developed prototype.

<b>Gross weight</b>	2.2 [kg]
<b>Number of rotors</b>	4
<b>Frame tilt range</b>	-90° to 90° (Total 180°)
<b>Rotor span at (0° tilt) (diagonal, length, width)</b>	500 [mm], 355 [mm], 355 [mm]
<b>Minimum rotor span (±90° tilt) (diagonal, length, width)</b>	410 [mm], 205 [mm], 355 [mm]
<b>Maximum rotor height offset (±90° tilt)</b>	150 [mm]

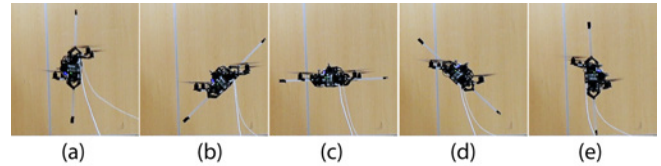


Fig. 7: Airframe tilt transition when the UAV is hovering. Tilt angles: (a) -90°, (b) -45°, (c) 0°, (d) 45°, (e) 90°.

the UAV through a wireless data stream and then to the ROS topic via a pose publisher node. Mavros then reads the feedback and sends it to the flight controller’s position control extended kalman filter (EKF).

#### IV. EXPERIMENTS

Experiments are carried out to test the tiltable airframe configurations of the developed prototype at various angles. An experiment is carried out to determine whether the UAV can tilt its airframe at various angles while flying and hover stably. The UAV is setup to take-off and hover in one spot. Then, in sequence, commands are sent to tilt the angle of the airframe. To observe the positioning accuracy for certain duration of hovering, a 5 s delay is provided between each angle adjustments. The experiment is performed with a varied tilting speed each time. The speed of the servo motors is controlled to set the tilting speed of the airframe. The sequence of various controllable tilt angles with a fixed heading is shown in Fig. 7. Rope support is used during the experiment on each side of the UAV for safety reasons in the event of a collision, however care is made to ensure that it does not interfere with flight tests.

The positioning and attitude holding accuracy during airframe tilting for a slower angle rate (10 rpm) and the attached servo’s maximum rate (45 rpm), can be seen in the graphs of Fig. 8 and Fig. 9. We can see the UAV’s position drift during the tilting instance in Fig. 8 with its  $[x, y, z]$  positions marked as  $[x_{slow}, y_{slow}, z_{slow}]$  and  $[x_{fast}, y_{fast}, z_{fast}]$  for slower and fast tilting case respectively. If the drift is too large, the UAV may collide with surrounding structure. Furthermore, the UAV’s attitude data with respect to the flight controller, with reference to the markings in Fig. 4(b), is recorded and presented in Fig. 9, which offers details on how the UAV is attempting to maintain the flight controller attached link’s (*link1*) attitude during the sudden change in balance and attitude change during tilt, particularly at higher rates. In Fig. 9, the roll, pitch, yaw values are marked as  $[\phi_{slow}, \theta_{slow}, \psi_{slow}]$  and  $[\phi_{fast}, \theta_{fast}, \psi_{fast}]$  for slower and fast tilting cases respectively.

Another experiment is carried out to observe the motion of the UAV when tilted at various angles. To perform the test, four setpoint positions are provided in succession to guide the UAV autonomously through a square pattern. For flight testing, only the four vertices are sent with an acceptable position error of 0.15 m. The experiment is repeated for varying airframe tilt angles while following through all four setpoints. The position information of the UAV during the experiment is shown in Fig. 10. It can be seen that the tilted UAV may safely maneuver in a given direction.

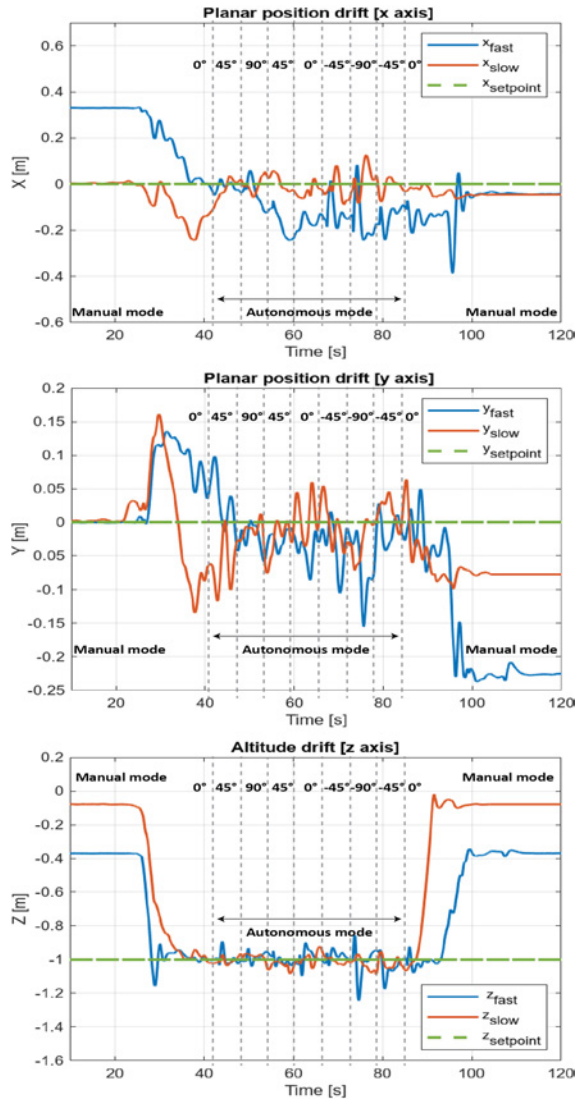


Fig. 8: Position drift of the hovering UAV during airframe tilt transition control.

## V. DISCUSSIONS AND FUTURE WORKS

In this research, we developed a tiltable airframe UAV prototype and observed that the UAV can fly stably even when the airframe is tilted and rotor heights change. However, regardless of height change, it is critical that all rotors are in upright parallel configuration. In the prototype, we employed two servo motors to achieve airframe tilting. During tilt angle control, these motors should be in synchrony at all times. Furthermore, if a parallel link mechanism is used in the future, the number of joint actuating servos may be decreased to one, posing less of an issue for angle change synchronization and servo motor type.

In the first experiment, the tilt angle is changed at two different speed while the position of the UAV is kept at a holding point. Fig. 9 shows the attitude measured throughout the two flights. At the instance of tilt transition, pitch angle can be seen changing proportionally to the speed of tilt. The direction of the pitch change suggests that the pitch rate is mainly induced by the moment caused by rotation

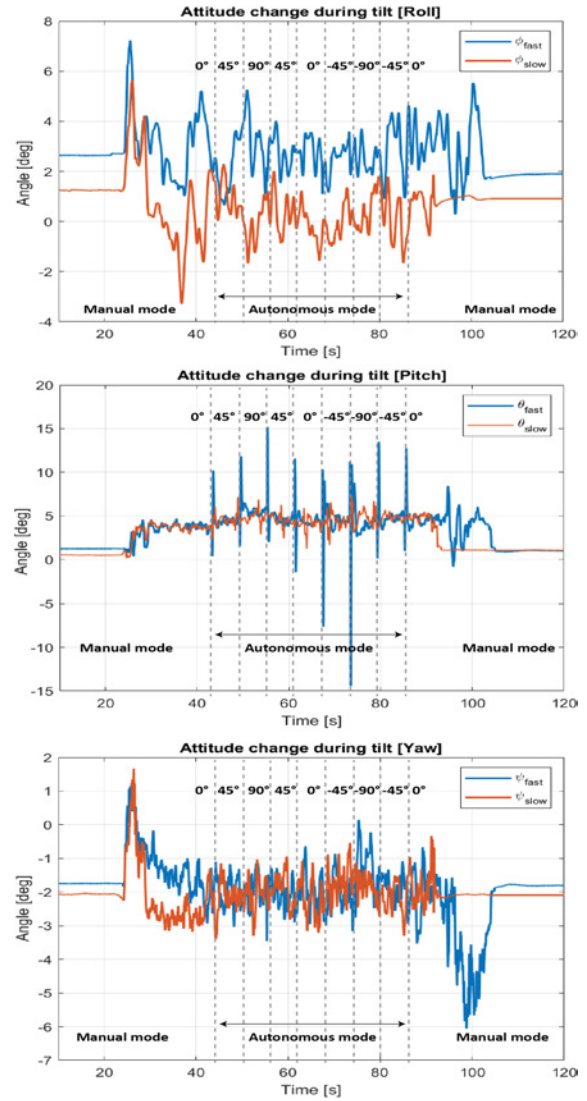


Fig. 9: Attitude response of the hovering UAV during airframe tilt transition control.

of the servo motors during configuration change. The flight controller is able to keep the attitude level without losing control, even in the case of rapidly changing tilt angles.

During the same experiment, the ability of position holding is evaluated. In Fig. 8, large change in x-axis (marked in Fig.4), namely the front-facing axis, is observed. The drift is proportional to the pitch change induced by tilt adjustment. No major change can be observed in y-axis, namely the right-facing axis. In z-axis, namely the altitude, small changes can be observed in slow tilt rate, while some considerable change can be observed in fast tilt rate. The flight controller can be seen to effectively rectify these drifts. Furthermore, some constant error from the setpoint in position holding in the level plane, x-axis and y-axis, can be observed due to the repeatedly changing tilt angle. The frequency of tilt change is so persistent such that the flight controller's position control does not have adequate time to follow the exact setpoint position resulting in some small error.

In the setpoint position experiment shown in Fig. 10,

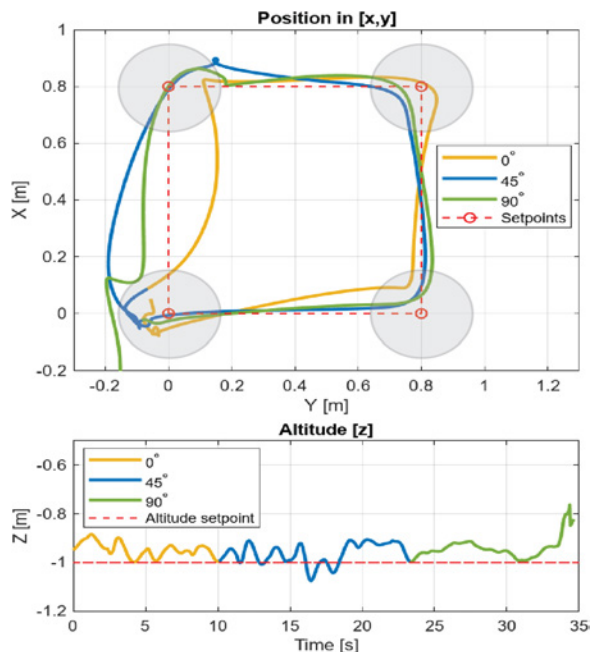


Fig. 10: Waypoint position control with different tilted configurations.

the experiment result shows that waypoint following performance of each tilting configuration are arguably similar. Each waypoint is followed correctly with little to moderate drift even when the tilt angle is changed. Additionally, the altitude data shows no major sink or raise at the moment the configuration angle is changed. Still, the performance of altitude keeping in 90° configuration seems to be slightly reduced compared to other configurations.

The servo motor maximum tilt rate of 45 rpm have been tested in a separate experiment. Several continuous 0 to 90° tilts at the maximum speed are tested, the experiment shows that UAV remains controllable at such high speed tilt. According to our understanding, this is the fastest tilting speed ever achieved for a tiltable airframe UAV while hovering in a fixed position. A video demonstration is available at <https://youtu.be/hvaMAyjFY2c>. Due to the speed limitation of the servo motor, faster than 45 rpm tilt rate was not able to be tested. Further test of increased tilting speed is expected in the future work.

## VI. CONCLUSIONS

A tiltable airframe UAV is designed to allow its body to be tilted in various directions while also enabling a manipulator tip attached to the airframe to be inclined in various directions. The tilting of the airframe is accomplished by angling the rotors while maintaining them upright and parallel to one other at all times. We demonstrate that the UAV can hover in a fixed position and fly safely at various tilt angles using flight experiments. Because the tilting airframe serves as the manipulator body, it may be employed in aerial manipulation applications that need a longer manipulator design. If the appropriate equipment is mounted to the manipulator ends, it may be utilized for aerial inspection tasks at high reach locations.

## ACKNOWLEDGMENT

This work was partially supported by JST, CREST Grant Number JPMJCR22C1, Japan.

## REFERENCES

- [1] H. B. Khamseh, F. Janabi-Sharifi, and A. Abdessameud, "Aerial manipulation—a literature survey," *Robotics and Autonomous Systems*, vol. 107, pp. 221–235, 2018.
- [2] R. Ashour, T. Taha, F. Mohamed, E. Hableel, Y. A. Kheil, M. Elsalamouny, M. Kadadha, K. Rangan, J. Dias, L. Seneviratne *et al.*, "Site inspection drone: A solution for inspecting and regulating construction sites," in *2016 IEEE 59th International midwest symposium on circuits and systems (MWSCAS)*. IEEE, 2016, pp. 1–4.
- [3] J. Seo, L. Duque, and J. Wacker, "Drone-enabled bridge inspection methodology and application," *Automation in construction*, vol. 94, pp. 112–126, 2018.
- [4] Y. Liu, J. Shi, Z. Liu, J. Huang, and T. Zhou, "Two-layer routing for high-voltage powerline inspection by cooperated ground vehicle and drone," *Energies*, vol. 12, no. 7, p. 1385, 2019.
- [5] J. F. Falorca and J. C. G. Lanzinha, "Facade inspections with drones—theoretical analysis and exploratory tests," *International Journal of Building Pathology and Adaptation*, vol. 39, no. 2, pp. 235–258, 2021.
- [6] F. Ruggiero, V. Lippiello, and A. Ollero, "Introduction to the special issue on aerial manipulation," *IEEE Robotics and Automation Letters*, vol. 3, no. 3, pp. 2734–2737, 2018.
- [7] A. Ollero, M. Tognon, A. Suarez, D. Lee, and A. Franchi, "Past, present, and future of aerial robotic manipulators," *IEEE Transactions on Robotics*, vol. 38, no. 1, pp. 626–645, 2021.
- [8] R. Ladig, H. Paul, R. Miyazaki, and K. Shimonomura, "Aerial manipulation using multirotor uav: a review from the aspect of operating space and force," *Journal of Robotics and Mechatronics*, vol. 33, no. 2, pp. 196–204, 2021.
- [9] H. Paul, R. Miyazaki, R. Ladig, and K. Shimonomura, "Tams: development of a multipurpose three-arm aerial manipulator system," *Advanced Robotics*, vol. 35, no. 1, pp. 31–47, 2021.
- [10] H. Paul, R. R. Martinez, R. Ladig, and K. Shimonomura, "Lightweight multipurpose three-arm aerial manipulator systems for uav adaptive leveling after landing and overhead docking," *Drones*, vol. 6, no. 12, p. 380, 2022.
- [11] M. Kamel, S. Verling, O. Elkhatib, C. Sprecher, P. Wulkop, Z. Taylor, R. Siegwart, and I. Gilitschenski, "The voliro omniorientational hexacopter: An agile and maneuverable tiltable-rotor aerial vehicle," *IEEE Robotics & Automation Magazine*, vol. 25, no. 4, pp. 34–44, 2018.
- [12] M. Xie and Z. Tian, "A review on pipeline integrity management utilizing in-line inspection data," *Engineering Failure Analysis*, vol. 92, pp. 222–239, 2018.
- [13] R. A. Mattar and R. Kalai, "Development of a wall-sticking drone for non-destructive ultrasonic and corrosion testing," *Drones*, vol. 2, no. 1, p. 8, 2018.
- [14] K. Alexis, C. Huerzeler, and R. Siegwart, "Hybrid modeling and control of a coaxial unmanned rotorcraft interacting with its environment through contact," in *2013 IEEE International Conference on Robotics and Automation*. IEEE, 2013, pp. 5417–5424.
- [15] C. Papachristos, K. Alexis, and A. Tzes, "Efficient force exertion for aerial robotic manipulation: Exploiting the thrust-vectoring authority of a tri-tiltrotor uav," in *2014 IEEE international conference on robotics and automation (ICRA)*. IEEE, 2014, pp. 4500–4505.
- [16] R. Miyazaki, H. Paul, T. Kominami, R. R. Martinez, and K. Shimonomura, "Flying washer: Development of high-pressure washing aerial robot employing multirotor platform with add-on thrusters," *Drones*, vol. 6, no. 10, p. 286, 2022.
- [17] P. Zheng, X. Tan, B. B. Kocer, E. Yang, and M. Kovac, "Tilt-drone: A fully-actuated tilting quadrotor platform," *IEEE Robotics and Automation Letters*, vol. 5, no. 4, pp. 6845–6852, 2020.
- [18] C. Ding and L. Lu, "A tilting-rotor unmanned aerial vehicle for enhanced aerial locomotion and manipulation capabilities: Design, control, and applications," *IEEE/ASME Transactions on Mechatronics*, vol. 26, no. 4, pp. 2237–2248, 2020.
- [19] A. Sakaguchi and K. Yamamoto, "A novel quadrotor with a 3-axis deformable frame using tilting motions of parallel link modules without thrust loss," *IEEE Robotics and Automation Letters*, vol. 7, no. 4, pp. 9581–9588, 2022.